JurnalPolimesin
Department of Mechanical Engineering
State Polytechnic of Lhokseumawe
http://e-jurnal.pnl.ac.id/polimesin
e-ISSN : 2549-1999 No. : 1 Month : February
p-ISSN : 1693-5462 Volume : 22 Year : 2024

Article Processing Dates: Received on 2023-11-22, Reviewed on 2023-11-28, Revised on 2023-12-18, Accepted on 2023-12-28 and Available online on 2024-02-29

Analysis Of Helical Gear Failure In Off-Road 4×4 Gearbox

Husaini*, Haris Darmawan, Nurdin Ali
Department of Mechanical Engineering, Universitas Syiah Kuala, Banda Aceh, 23111, Indonesia
*Corresponding author: husainiftm@usk.ac.id

Abstract

Surface failure is evident in helical gear in off-road 4×4 gearbox,requiring the identification ofroot causes. Therefore, this study aimed to explore the factors contributing to helical gearfailure in off-road 4×4 vehicles. Initially, crack in helical gear wascaused by manufacturing or material defects during production or the heat treatment process, manifesting as inhomogeneities in the microstructure or other imperfections. Crack propagation possibly occurred due to continuous stress during off-road 4×4 usage, influenced by factors such as excessive loads, vibrations, or extreme off-road conditions.The exploration process began with a comprehensive set of analyses, including visual observation, hardness testing, chemical composition analysis, microstructure testing, and stress analysis. Subsequently, the material composition of gear was identified as high-carbon steel meeting AISI 1080 standards. Although the average surface hardness value was 95.49 HRB, which was slightly lower than AISI 1080, the microstructure comprised pearlite and cementite. Surface fracture observations revealedinitial crackthat propagated, leading to brittle fractures. The average stress intensity factor (K_I)was alsomeasured 54.65 MPa.m$^{1/2}$, which surpassed fracture toughness value (K_{IC}) of AISI 1080 steel at 45.5 MPa.m$^{1/2}$.In conclusion, helical gear failure was directly attributed to the propagation of initial crack, thereby resulting in fractures.

Keywords:
Helical gears, failure analysis, finite element method.

1 Introduction

Gear is mechanical device used for transmitting rotational motion in an engine. By applying straight-cut and helical gear in gearbox, these transmission systems are widely used in industrial equipment due to the high efficiency, availability in various ratios, and ease of identification and repair [1][2].Gearbox, composed of closely arranged multiple gear, facilitates the transmission of rotational movement between engine shafts, adjusting the rotation speed as needed [3]. The operational principle comprises transferring rotation from the motor to the input shaft and then to the main shaft. Subsequently, the torque of the main shaft is transmitted to the machine spindle. The torque of the main shaft is transferred to the machine spindle while the output shaft produced by the motor varies depending on the desired RPM, which is influenced by the shape of gear and the ratios [4].

Gear often faces failure, leading to direct losses attributed to design errors, material defects, maintenance mistakes, high surface contact stresses, improper lubrication, and misalignment [5]. For example, in off-road 4×4 engine, one of helical gears in gearbox experienced severe surface damage due to heavy loads and inadequate lubrication [6].Although helical gear is designed for a 4-year lifespan, it broke down after only 2 years of use. Insufficient maintenance and frequent operation on rough roads contributed to gear premature failure. Prior investigation by Husaini et al. suggested that gear failure resulted from initial crack and impacted loads in rough terrain [7]. Boonmag V mentioned that gear failure started from crack on the outer surface, leading to a combination of brittle and ductile fractures with a microstructure comprising ferrite and pearlite [8].

Numerous studies investigated the causes of gear failure, showing that failure occurred when stress intensity factor surpasses fracture toughness value [9]. Continuous operation induces initial crack, leading to failure [10], while dynamic loads cause fatigue [11], and shear stress exceeding the limit results in failure [12]. Consequently, thiscurrent study aims to identify the causes of failure in helical gear, enabling the anticipation of similar failure.

2 Study Methodology

Helical gear was crafted from high-carbon steel, in accordancewith AISI 1080 standards [12]. Fig. 1 showed the helical gear failure, which indicated surface damage.

Fig. 1. Helical gear failure.

Thisstudy began with a visual examination of helical gear, followed by hardness testing, chemical composition analysis, microstructure testing, and stress analysis using Finite Element Method (FEM). The resulting stress data were used to calculate stress intensity factor around crack tip.

2.1 Hardness Testing using ASTM E18 Standard

Initiated by cutting a sample close to the fracture surface on the helical gear, hardness testing points were shown in Fig. 2. The sample was then ground to achieve a flat surface, with testing conducted on both outer and inner surfaces to ascertain uniform hardness. Rockwell hardness testing, following ASTM E18 standards, used a Zwick/Roell ZHV 10-type tool.

2.2 Chemical Composition Testing

Chemical composition testing was performed to identify the chemical elements and the quantities in the material. The results were used as references to determine the appropriate material standard group. Furthermore, the resultswere compared with material standards to determine whether the material used complied with the standards or not. Chemical composition testing was conducted using Foundry Master UV spectrometer.

2.3 Microstructure Observation

The microstructure observation process started with grinding the specimen finely using sandpaper, followed by etching the specimen surface with HCL and alcohol before observation using an Olympus BX41M optical microscope. The test was conducted to observe the characteristics of grains and phases present in gear. To determine grain boundaries, the etchant used was a mixture of

HCL and alcohol in a 2:1 ratio. As a result, microstructure was observed at magnifications of 200x and 500x.

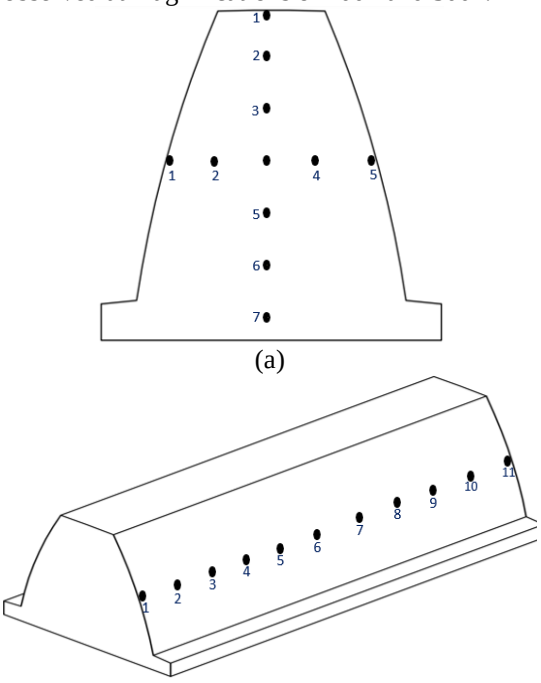

Fig. 2. Hardness testing points, (a) center part, (b) side part.

2.4 Fracture Surface Observation

Fractography and microscopic structure observation of the fractured gear used SEM to locate initial crack, analyze microscopic structures, and provide fatigue information. SEM procedures included specimen cutting, coating with a conductive layer, mounting on an SEM holder, electrically charging the sample, electron scanning, and signal use to create a high-resolution three-dimensional image of the sample surface [13].

2.5 Modeling and Stress Analysis using Finite Element Method (FEM)

Gear geometry modeling in Autodesk Inventor software consistedof two types, namely a flawless model and a model with initial crackshown in Fig. 3.

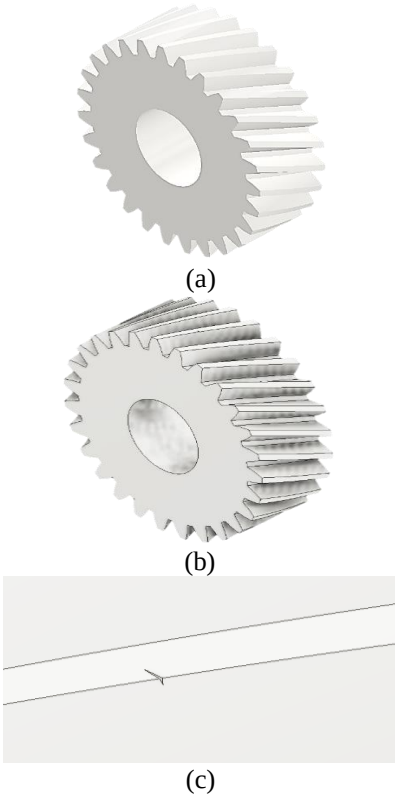

Fig. 3. (a) Model without crack, (b) model with initial crack, (c) enlarged defect area.

The preprocessing comprised two stages, and the first comprised inputting material properties for AISI 1080. In the second stage, a load of 898 N, derived from gear force calculations, was applied. Boundary conditions were determined, as shown in Fig. 4.

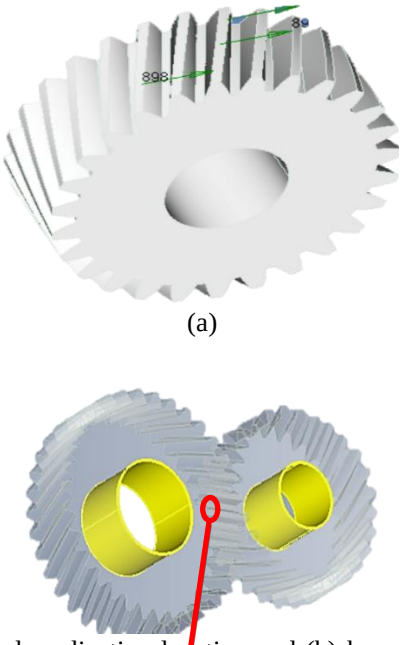

Fig. 4. (a) Load application location and (b) boundary condition determination location.

Meshing divided a 3D model into discrete domains, significantly influencing simulation accuracy. Smaller mesh settings produced simulation results closer to actual values. Meshing, shown in Fig. 5, subdivided gear model into smaller elements.

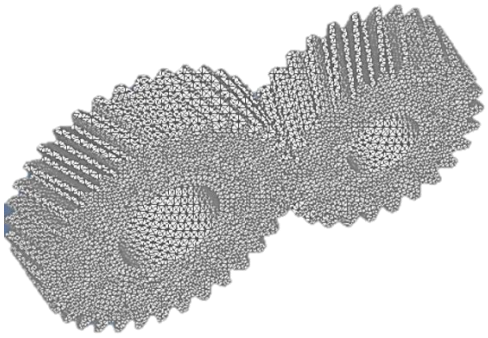

Fig. 5. Meshing results on gear.

The final step in using FEMAP application for analytical setup was to determine the numerical solution. This process duration depended on the mesh size used. The result shown in color contours represented stress values on gear.

2.6 Calculation of Stress Intensity Factor

Stress intensity factor, crucial for determining crack propagation, was calculated using stress from simulation results. Eq. 1 determined stress intensity factor (K_I) around crack tip.

$$K_I = \frac{\sigma_{xx} \cdot \sqrt{2\pi r}}{\left(\cos\frac{\theta}{2}\right)\left[1-\sin\left(\frac{\theta}{2}\right)\sin\left(\frac{3\theta}{2}\right)\right]} \quad (1)$$

Where:

σ_{xx} = stress (MPa)
r =distance from crack tip to the nodes point (m)
θ = angle from the nodes point to the X-axis (°)
K_I =stress intensity factor (MPa.m$^{1/2}$)

3 Results and Discussion

3.1 Material Hardness

Hardness testing showed varying values near the outer and middle parts of gear surface, as presented in Fig. 6. The X-axis represented hardness in the vertical direction, and the Y-axis represented hardness in the horizontal direction as shown in Fig. 2.

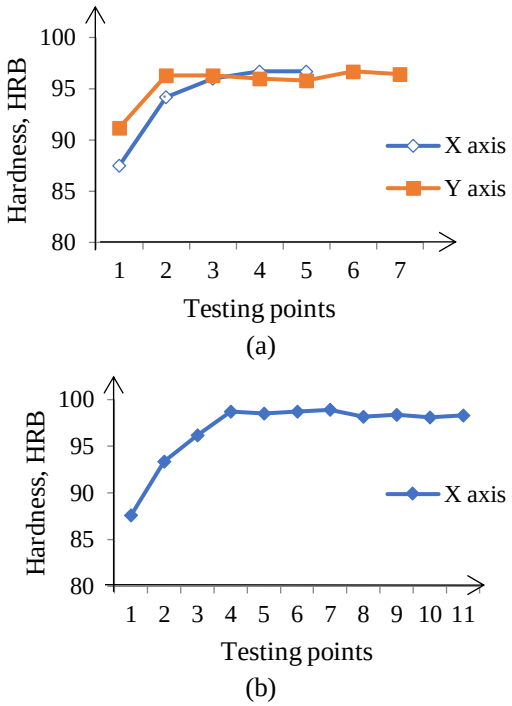

Fig. 6. Hardness testing results graph, (a) outer part, (b) side part.

The average hardness value from the test was 95.49 HRB, lower than AISI 1080's average hardness value of 99 HRB.

3.2 Chemical Composition

Helical gear contained medium carbon steel with properties including a 0.3%–0.8% carbon content and a ferrite and pearlite microstructure, providing strength but increased brittleness. Table 1 shows the test results.

Table 1. Chemical composition testing results

Elements	Test results	AISI 1080 standard[14]
Iron, Fe	85.8	98.13 – 98.65
Carbon, C	0.860	0.75 – 0.88
Manganese, Mn	0.696	0.60 – 0.90
Sulfur, S	0.0289	≤ 0.050
Phosphorous, P	0.0312	≤ 0.040

By knowing the material standard,then the mechanical properties of the material can be determined. AISI 1080's properties were shown in Table 2.

Table 2. Mechanical properties of AISI 1080 material [14]

Properties	Values	Units
Density (ρ)	7.85	g/cm^3
Ultimate strength (σ_B)	965	MPa
Yield strength (σ_{ys})	585	MPa
Bulk modulus (B)	160	GPa
Shear modulus (G)	80	GPa
Elastic modulus (E)	205	GPa
Poisson ratio (v)	0.29	-
Hardness, Rockwell B	99	HRB
Shear stress allowable	253.47	MPa

3.3 Microstructure

Microstructure testing, conducted using an Olympus BX41M optical microscope, was shown in Fig. 7.

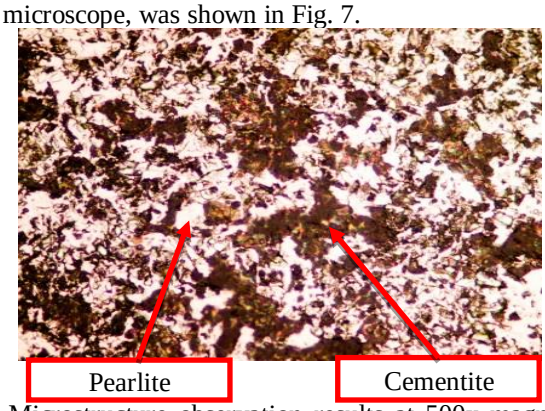

Fig. 7. Microstructure observation results at 500x magnification with pearlite and cementite microstructure.

3.4 Fracture Surface Observation

Visual observation showed that damage spanned more than half of the total gear profile. The fractured surface of the damaged gear was presented in Fig. 8, showing a brittle fracture pattern characterized by a granular appearance, light reflection, and occurrence in materials with a high carbon composition.

Fig. 8. Fractured surface due to failure.

SEM observation results, shown in Fig. 9, further described characteristics of brittle fracture, denoting a granular, shiny surface reflecting light, commonly found in materials with a high carbon composition.

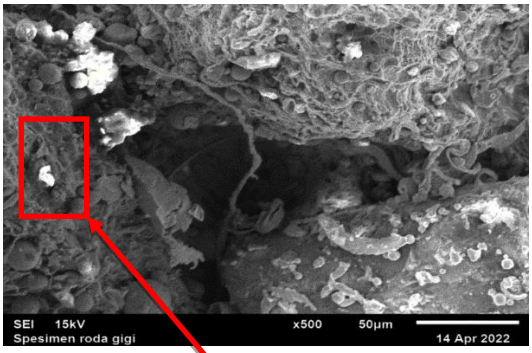

F ults.

3.5 Stress Intensity Factor

Stress analysis with initial cracksignified that the minimum von Mises stress was 43.22 MPa, while the maximum von Mises stress reached 691.5 MPa, as shown in Fig. 10(a).

Stress intensity factor (K_I) with initial crack could be calculated using Eq. 1. Fig. 10(b)showed the nodes points used to determine stress intensity factor, and the calculation results were shown in Table 3.

Stress intensity factor analysis (K_I) on helical gear with initial crack yielded average value of 54.65 MPa.m$^{1/2}$. Since fracture toughness value (K_{IC}) for AISI 1080 material was 45.5 MPa.m$^{1/2}$[15], it showed that crack propagated from initial crack to the final fracture, led to helical gear failure[16].

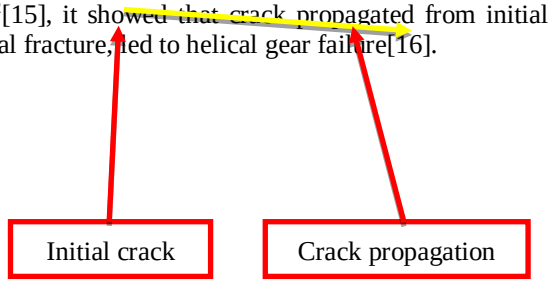

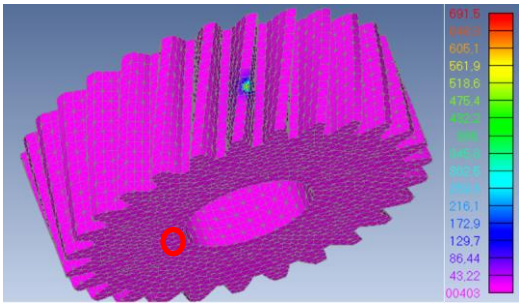

(a)

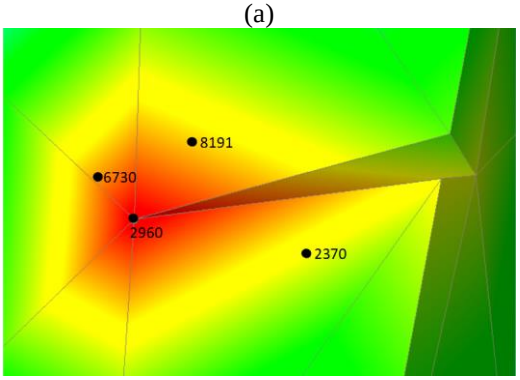

(b)

Fig. 10. (a) Simulation results with initial crack, (b) location of nodes points for stress intensity factoranalysis.

Table 3. Stress intensity factor (K_I) calculation

Nodes	σ (MPa)	r (m)	θ	K_I(MPa.m$^{1/2}$)
2370	550	0.00036	330	33.14
8191	570	0.00023	45	36.28
6730	645	0.00015	102	64.43
2960	690	0.00030	90	84.73
		Average		54.65

4 Conclusion

In conclusion, the results showed that the cause of helical gear failure was the presence of initial crack leading to crack propagation. This conclusion was further supported by stress intensity factor (K_I) analysis around crack tip, where the value exceeded fracturetoughness value (K_{IC}) standard for AISI 1080 material (K_I = 54.65 MPa.m$^{1/2}$>K_{IC} 45.5 MPa.m$^{1/2}$).

Acknowledgments

The authors are grateful to the UniversitasSyiah Kuala for their partly financial support through Research Grant No. 81/UN11.2.1/PT.01.03/PNBP/2023.

References

[1] H. Laitinen, A. Lajunen, and K. Tammi, “Improving electric vehicle energy efficiency with two-speed gearbox,” *2017 IEEE Veh. Power Propuls. Conf. VPPC 2017 - Proc.*, vol. 2018-January, pp. 1–5, Apr. 2018, doi: 10.1109/VPPC.2017.8330889.

[2] H. Wang, Z. Wang, and W. Liu, “Fault diagnosis of wind turbine gearbox based on vibration data,” *Proc. - 2018 IEEE 15th Int. Conf. E-bus. Eng. ICEBE 2018*, pp. 234–238, Dec. 2018, doi: 10.1109/ICEBE.2018.00045.

[3] Afenchenko, R. V., Barskii, V. A., Bashta, V. N., Kurdyumov, D. S., Malyar, A. V., & Ufimtsev, I. V., 2015. Development of the equipment for gearless gas-turbine power plants. *Russian Electrical Engineering*, Vol. 86, No. 10, pp. 576578.

[4] P. P. DIMAS, “ANALISIS PENYEBAB TERHAMBATNYA GERAK MAJUPADA GEARBOX DI KAPAL MV. SINAR JEPARA,” 2019, Accessed: Dec. 29, 2023. [Online]. Available: http://www.library.pip-semarang.ac.id

[5] H. Husaini and D. M. Dawud, “Numerical Analysis of Stress Causing Fracture Failure in the Gear Transmission System Applied on an Agricultural Machinery Equipment,” *J. Phys. Conf. Ser.*, vol. 1351, no. 1, p. 012021, Nov. 2019, doi: 10.1088/1742-6596/1351/1/012021.
[6] R. L. Mott, E. M. Vavrek, and J. Wang, *Machine Elements in Mechanical Design 6th Edition*. 2018.
[7] Husaini, D. M. Dawud, T. E. Putra, and N. Ali, “Failure analysis of spur gears used in transmission system applied on a hand tractor,” *Key Eng. Mater.*, vol. 841, pp. 144–149, 2020, doi: 10.4028/WWW.SCIENTIFIC.NET/KEM.841.144.
[8] V. Boonmag, O. Wisesook, A. Phukaoluan, and G. Pluphrach, “Micro-crack analyses of chromium steel JIS-SCr 420 for helical gear transmission,” *Key Eng. Mater.*, vol. 777 KEM, pp. 294–299, 2018, doi: 10.4028/WWW.SCIENTIFIC.NET/KEM.777.294.
[9] Husaini, T. E. Putra, and S. Novriandika, “Study of Failure Analysis of a Fracture Crankshaft Pulley Used on a Truck Engine,” *IOP Conf. Ser. Mater. Sci. Eng.*, vol. 739, no. 1, p. 012018, Jan. 2020, doi: 10.1088/1757-899X/739/1/012018.
[10] Husaini, R. Anshari, N. Ali, and J. Yunus, “The Analysis of the Failure of Leaf Spring Used as the Rear Suspension System in 110 PS Diesel Trucks,” *AIP Conf. Proc.*, vol. 2613, no. 1, Jan. 2023, doi: 10.1063/5.0119820/2866336.
[11] Husaini, A. Rizqullah, I. Hasanuddin, and M. Sadrawi, “The Failure Analysis of Crankshaft of Four Cylinder Diesel Engine Using Experimental Method,” *Key Eng. Mater.*, vol. 930, pp. 25–33, 2022, doi: 10.4028/P-II0E24.
[12] Husaini, Osama, and T. E. Putra, “The Analysis of Crankshaft Failure in a 2,500cc Diesel Engine Vehicle Using Experimental Method,” *Lect. Notes Mech. Eng.*, pp. 340–348, 2023, doi: 10.1007/978-981-19-3629-6_35.
[13] A. Abdullah and A. Mohammed, “Scanning Electron Microscopy (SEM): A Review,” *Proc. 2018 Int. Conf. Hydraul. Pneum. - HERVEX*, pp. 77–85, 2019.
[14] MatWeb. AISI 1080 Steel, as rolled. https://www.matweb.com/search/datasheet.aspx?matguid=37ca3458dfbe482fbe1efdf59d52e424&n=1&ckck=1, diakses pada tanggal 27 Juli 2023.
[15] O. G. Perveitalov, V. V. Nosov, A. M. Schipachev, and A. I. Alekhin, “Thermally Activated Crack Growth and Fracture Toughness Evaluation of Pipeline Steels Using Acoustic Emission,” *Met. 2023, Vol. 13, Page 1272*, vol. 13, no. 7, p. 1272, Jul. 2023, doi: 10.3390/MET13071272.
[16] T. L. Anderson, “FRACTURE MECHANICS: Fundamentals and Applications, Fourth Edition,” *Fract. Mech. Fundam. Appl. Fourth Ed.*, pp. 1–661, Jan. 2017, doi: 10.1201/9781315370293/FRACTURE-MECHANICS-TED-ANDERSON.